X-ray Studies of Self-Assembled Organic Monolayers Grown on Hydrogen-Terminated Si(111)

Hua Jin,[†] C. Reagan Kinser,[†] Paul A. Bertin,[‡] Donald E. Kramer,[†] Joseph A. Libera,[†] Mark C. Hersam,[†] Sonbinh T. Nguyen,[‡] and Michael J. Bedzyk*,[†]

Department of Materials Science and Engineering, and Nanoscale Science and Engineering Center, Northwestern University, Evanston, Illinois 60208, and Department of Chemistry and Nanoscale Science and Engineering Center, Northwestern University, Evanston, Illinois 60208

Received February 6, 2004. In Final Form: April 24, 2004

The structure of self-assembled monolayers (SAMs) of undecylenic acid methyl ester (SAM-**1**) and undec-10-enoic acid 2-bromo-ethyl ester (SAM-**2**) grown on hydrogen-passivated Si(111) were studied by X-ray reflectivity (XRR), X-ray standing waves (XSW), X-ray fluorescence (XRF), atomic force microscopy, and X-ray photoelectron spectroscopy (XPS). The two different SAMs were grown by immersion of H−Si(111) substrates into the two different concentrated esters. UV irradiation during immersion was used to create Si dangling bond sites that act as initiators of the surface free-radical addition process that leads to film growth. The XRR structural analysis reveals that the molecules of SAM-**1** and SAM-**2** respectively have area densities corresponding to 50% and 57% of the density of Si(111) surface dangling bonds and produce films with less than 4 Å root-mean-square roughness that have layer thicknesses of 12.2 and 13.2 Å. Considering the molecular lengths, these thicknesses correspond to a 38° and 23° tilt angle for the respective molecules. For SAM-**2**/Si(111) samples, XRF analysis reveals a 0.58 monolayer (ML) Br total coverage. Single-crystal Bragg diffraction XSW analysis reveals (unexpectedly) that 0.48 ML of these Br atoms are at a Si(111) lattice position height that is identical to the T_1 site that was previously found by XSW analysis for Br adsorbed onto Si(111) from a methanol solution and from ultrahigh vacuum. From the combined XPS, XRR, XRF, and XSW evidence, it is concluded that Br abstraction by reactive surface dangling bonds competes with olefin addition to the surface.

Introduction

The growth of self-assembled monolayers (SAMs) directly on silicon surfaces has been the subject of much interest in recent years. Stable, functionalized, and densely packed monolayers of organic molecules covalently bonded to silicon surfaces have numerous potential applications in hybrid electronic and sensing devices, biotechnology, and soft lithography.[1−4] Since the operation of such sensors is strongly dependent on the conformation and uniformity of the organic monolayer, sophisticated characterization strategies are needed to provide a detailed atomic-scale picture of the resulting interface and ultrathin film structure.

Covalently modified silicon surfaces have been prepared via catalyzed,[4] thermal,[4,5] and photochemical[6] reaction of hydrogen-passivated silicon with terminal alkenes. Monolayer growth occurs on the surface by a free radical addition process initiated at Si dangling bonds (Figure 1). Using this approach for monolayer growth, SAMs of omega-functionalized terminal alkenes exhibiting alkyl,[4,5,7] ester,[5,8] or amine[9−11] moieties have been demonstrated. Further, wet chemical strategies have been developed to terminate these surfaces with a diverse range of functionalities, including dendrimers and DNA.[7−10,12]

X-ray reflectivity (XRR),[4,5,13−15] X-ray photoelectron spectroscopy (XPS),[4,6−11] secondary ion mass spectroscopy (SIMS),[16,17] Fourier transform infrared (FTIR) spectroscopy,[4−6,11] and ellipsometry[4,6,7] have been used extensively for characterizing the physical and chemical structure of SAMs on silicon surfaces. Each of these tools readily

* Corresponding author. Address: Northwestern University, Materials Science Department, 2220 Campus Drive, Evanston, IL 60208. Tel: (847) 491-3570. Fax: (847) 467-2269. E-mail: bedzyk@northwestern.edu.

[†] Department of Materials Science and Engineering, and Nanoscale Science and Engineering Center.

[‡] Department of Chemistry and Nanoscale Science and Engineering Center.

(1) Wolkow, R. A. *Annu. Rev. Phys. Chem.* **1999**, *50*, 413.
(2) Jeon, N. L.; Finnie, K.; Branshar, K.; Nuzzo, R. G. *Langmuir* **1997**, *13*, 3382.
(3) Buriak, J. M. *Chem. Rev.* **2002**, *102*, 1272.
(4) Linford, M. R.; Fenter, P.; Eisenberger, P. M.; Chidsey, C. E. D. *J. Am. Chem. Soc.* **1995**, *117*, 3145.
(5) Sieval, A. B.; Demirel, A. L.; Nissink, J. W. M.; Linford, M. R.; Maas, J. H. van der; Jeu, W. H. de; Zuilhof, H.; Sudhölter, E. J. R. *Langmuir* **1998**, *14*, 1759.
(6) Cicero, R. L.; Linford, M. R.; Chidsey, C. E. D. *Langmuir* **2000**, *16*, 5688.
(7) Wagner, P.; Nock, S.; Spudich, J. A.; Volkmuth, W. D.; Chu, S.; Cicero, R. L.; Wade, C. P.; Linford, M. R.; Chidsey, C. E. D. *J. Struct. Biol.* **1997**, *119*, 189.
(8) Strother, T.; Cai, W.; Zhao, X.; Hamers, R. J.; Smith, L. M. *J. Am. Chem. Soc.* **2000**, *122*, 1205.
(9) Lin, Z.; Strother, T.; Cai, W.; Cao, X.; Smith, L. M.; Hamers, R. J. *Langmuir* **2002**, *18*, 788.
(10) Strother, T.; Hamers, R. J.; Smith, L. M. *Nucleic Acids Res.* **2000**, *28*, 3535.
(11) Sieval, A. B.; Linke, R.; Heij, G.; Meijer, G.; Zuilhof, H.; Sudhölter, E. J. R. *Langmuir* **2001**, *17*, 7554.
(12) Cicero, R. L.; Wagner, P.; Linford, M. R.; Hawker, C. J.; Waymouth, R. M.; Chidsey, C. E. D. *Polym. Prepr.* (*Am. Chem. Soc., Div. Polym. Chem.*) **1997**, *38*, 904.
(13) Rabedeau, T. A.; Tidswell, I. M.; Pershan, P. S.; Bevk, P. S. J.; Freer, B. S. *Appl. Phys. Lett.* **1991**, *59*, 3422.
(14) Tidswell, I. M.; Ocko, B. M.; Pershan, P. S.; Wasserman, S. R.; Whitesides, G. M.; Axe, J. D. *Phys. Rev. B* **1990**, *41*, 1111.
(15) Als-Nielsen, J.; McMorrow, D. *Elements of Modern X-ray Physics*; John Wiley & Sons Ltd.: Chichester, U.K., 2001; Chapter 3, pp 73−92.
(16) Benninghoven, A.; Rüdenauer, F. G.; Werner, H. W. *Secondary Ion Mass Spectroscopy*: *Basic Concepts, Instrumental Aspects, Applications and Trends*; John Wiley & Sons: New York, 1987; Chapter 5, p 691.
(17) Lua, Y.-Y.; Niederhauser, T. L.; Matheson, R.; Bristol, C.; Mowat, I. A.; Asplund, M. C.; Linford, M. R. *Langmuir* **2002**, *18*, 4840.

10.1021/la0496690 CCC: $27.50
Published on Web 06/03/2004

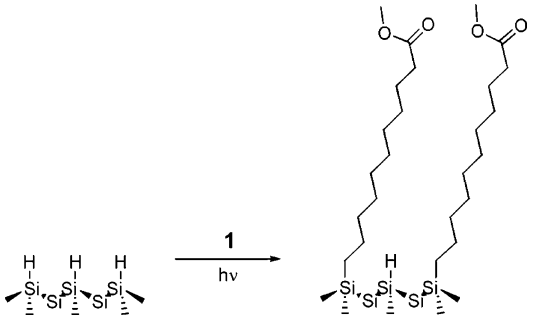

Figure 1. Schematic representation of the process to prepare SAM-**1**.

Chart 1. Schematic Drawing of Molecules 1 (Undecylenic Acid Methyl Ester), 2 (Undec-10-enoic Acid 2-Bromo-ethyl Ester), and 3 (Undecanoic Acid 2-Bromo-ethyl Ester)

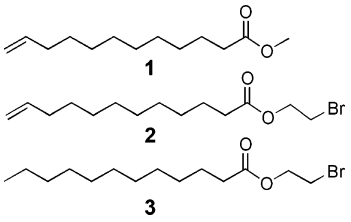

provides a direct measure of either the chemical (XPS, SIMS, FTIR) *or* physical (XRR, ellipsometry) structure of the SAM, but obtaining a composite atomic-scale picture can require indirect analyses which suffer from the inherent limitations of assumptions made in the various models.[5,6] In this report, we introduce the use of single-crystal X-ray standing waves (XSW) to simultaneously measure the physical *and* chemical structure of a SAM covalently bound on the Si(111) surface. The single-crystal XSW technique, which monitors a characteristic atomic X-ray fluorescence signal while scanning in angle through a Bragg peak of the single crystal, is used to locate the position (adsorbate height) of that atom relative to the single-crystal lattice planes.[18,19]

In our present study, undecylenic acid methyl ester (**1**, Chart 1) was selected as a model system, and undec-10-enoic acid 2-bromo-ethyl ester (**2,** Chart 1) was chosen as a complimentary system with Br acting as an ideal X-ray fluorescence tag atom. We grew SAMs of **1** (SAM-**1**) and **2** (SAM-**2**) on hydrogen-passivated Si(111) and employed a variety of X-ray techniques for analyzing the resulting structures. The film thickness, interface roughness, and chain packing density were characterized by XRR. For SAM-**2**, the Br area density was determined by X-ray fluorescence (XRF). Single-crystal XSW analysis was used to determine the Br position relative to the Si(111) lattice planes. To our knowledge, this is the first XRR or XSW report on the nanoscale structure of monolayers of **1** or **2** on the Si(111) surface.

Experimental Section

General Information. All chemicals were reagent grade or the highest available commercial grade and used as received unless otherwise specified. Ultrapure 18 MΩ cm water was obtained from a NANOpure Diamond Life Science (UV/UF) ultrapure water system (Barnstead/Thermolyne, Dubuque, IA). Other materials were obtained as follows: undecylenic acid methyl ester (**1**) (96%) (Sigma-Aldrich), 5% palladium on activated carbon powder (Degussa), Si(111) wafers (Virginia Semiconductor).

^{1}H and ^{13}C NMR spectra were recorded on a Varian INOVA 500 FT-NMR spectrometer (500 MHz for ^{1}H NMR, 125 MHz for ^{13}C NMR). ^{1}H NMR data are reported as follows: chemical shift {multiplicity (b = broad, s = singlet, d = doublet, t = triplet, q = quartet, qn = quintet, and m = multiplet), integration, and peak assignments}. ^{1}H and ^{13}C chemical shifts are reported in ppm downfield from tetramethylsilane (TMS). Gas chromatography (GC) analyses were carried out on a Hewlett-Packard 5890A instrument equipped with a FID detector interfaced to an HP3396A integrator. The instrument was fitted with a 30-m HP-5 capillary column with a 0.32-mm inner diameter and a 0.25-μm film thickness. The flow rate was 1.8 mL/min. High-resolution electron impact mass spectrometry (HREIMS) data were obtained on a VG 70-SE instrument. Elemental analyses were provided by Atlantic Microlab, Inc. (Norcross, GA).

Synthesis of Undec-10-enoic Acid 2-Bromo-ethyl Ester (2). In a 250-mL round-bottom flask was added undecylenic acid methyl ester (8.80 g, 44.5 mmol), 2-bromoethanol (3.78 mL, 53.4 mmol), and *p*-toluenesulfonic acid monohydrate (844 mg, 4.45 mmol). Benzene (50 mL) was added, and a Dean-Starck trap was fitted to the top of the flask. A water-cooled condenser was placed on top of the Dean-Starck trap, and the resulting mixture was heated to reflux. Over a period of 24 h, the reaction volume was reduced to 30 mL by occasionally decanting solvent from the bottom of the Dean-Starck trap. The reaction was cooled to room temperature, and the solvent was removed in vacuo. The crude product was dissolved in ether (200 mL) and washed with brine (3 × 50 mL). The organic fraction was collected, dried over sodium sulfate, filtered, and concentrated to afford crude yellow oil. Purification of the residue on silica using 30% hexanes in CH_2Cl_2 as an eluent yielded the desired product **2** as a clear oil (8.95 g, 30.7 mmol, 69%). ^{1}H NMR ($CDCl_3$): δ 1.30−1.37 (m, 10H, $CH_2(CH_2)_5CH_2$), 1.64 (m, 2H, CH_2CH_2CO), 2.04 (m, 2H, $CHCH_2$), 2.35 (t, 2H, J = 8 Hz, CH_2CO), 3.51 (t, 2H, J = 6 Hz, $BrCH_2$), 4.39 (t, 2H, J = 6 Hz, $COOCH_2$), 4.96 (m, 2H, CH_2CH), 5.81 (m, 1H, CH_2CHCH_2). ^{13}C NMR ($CDCl_3$): δ 25.07, 29.02, 29.07, 29.23, 29.26, 29.37, 29.46, 33.97, 34.29, 63.78, 114.35, 139.36, 173.55. HREIMS: Calcd for $C_{13}H_{23}BrO_2$, 290.0876. Found, 290.0876. Anal. Calcd for $C_{13}H_{23}BrO_2$: C, 53.61; H, 7.96. Found: C, 53.71; H, 8.04.

Synthesis of Undecanoic Acid 2-Bromo-ethyl Ester (3). In a 100-mL round-bottom flask was added **2** (1.00 g, 3.43 mmol), 5% Pd/C powder (75 mg), methanol (5 mL), and CH_2Cl_2 (10 mL). The mixture was stirred at room temperature and degassed with H_2 (1 atm) from a charged balloon for 20 min. The reaction was left under a positive pressure of H_2 (1 atm) for 24 h. The catalyst was removed by filtering through Celite, and the solvent was removed in vacuo to yield crude yellow oil. Purification of the residue on silica using 30% hexanes in CH_2Cl_2 as an eluent yielded the desired product **3** as a clear oil (755 mg, 2.58 mmol, 75%). ^{1}H NMR ($CDCl_3$): δ (m, 10H, $CH_2(CH_2)_5CH_2$), 1.64 (m, 2H, CH_2CH_2CO), 2.04 (m, 2H, $CHCH_2$), 2.35 (t, 2H, J = 8 Hz, CH_2CO), 3.51 (t, 2H, J = 6 Hz, $BrCH_2$), 4.39 (t, 2H, J = 6 Hz, $COOCH_2$), 4.96 (m, 2H, CH_2CH), 5.81 (m, 1H, CH_2CHCH_2). ^{13}C NMR ($CDCl_3$): δ 25.07, 29.02, 29.07, 29.23, 29.26, 29.37, 29.46, 33.97, 34.29, 63.78, 114.35, 139.36, 173.55. HREIMS: Calcd for $C_{13}H_{23}BrO_2$, 290.0876. Found, 290.0876. Anal. Calcd for $C_{13}H_{23}BrO_2$: C, 53.61; H, 7.96. Found: C, 53.71; H, 8.04.

Cleaning and Etching of Silicon. Single-side polished, 0.5 mm thick, silicon (111) wafers (n-type, 0.01 Ω cm, <0.25° miscut) were rinsed with acetone and propanol and subjected to a hydrogen passivation treatment.[20] Specifically, the native oxide surface was removed by a 15-s immersion in 0.5% HF followed by rinsing with ultrapure 18 MΩ cm water. The wafers were immersed in a 4:1 (v/v) H_2SO_4/30% H_2O_2 (aq) for 10 min at 90 °C to remove organic contaminants. For hydrogen passivation, the clean silicon wafers were then immersed for 15 min in a 40% clean-room-grade NH_4F (aq) which had been partially deoxygenated by argon sparging. The wafers were rinsed between and after each step in ultrapure water. Hydrogen passivation of the

(18) Golovchenko, J. A.; Patel, J. R.; Kaplan, D. R.; Cowan, P. L.; Bedzyk, M. J. *Phys. Rev. Lett.* **1982**, *49*, 560.

(19) For a review of XSW see: Bedzyk, M. J.; Cheng, L. *Rev. Mineral. Geochem.* **2002**, *49*, 221.

(20) Higashi, G. S.; Chabal, Y. J.; Trucks, G. W.; Raghavachari, K. *Appl. Phys. Lett.* **1990**, *12*, 656.

silicon surfaces was confirmed by XPS[21] and by measuring the silicon bilayer step height (3.1 Å) with atomic force microscopy (AFM). The H−Si(111) wafers were stored in a nitrogen glovebox for 1−2 days until used.

Monolayer Preparation. All monolayer preparations were performed in the nitrogen glovebox. Monolayers of **1**, **2**, and **3** (SAM-**1**, SAM-**2**, and SAM-**3**, respectively) were prepared following the procedure of Strother et al.[8] A thin layer (less than 1 mm) of the neat compound was pipetted onto the H−Si(111) surface so that it was fully covered. The sample was then exposed to 254 nm UV light for 2 h. Samples were then rinsed thoroughly in CH_2Cl_2 and ultrasonicated for 15 min in CH_2Cl_2 and methanol. Samples were stored in the nitrogen glovebox prior to analysis.

Time-of-Flight Secondary-Ion Mass Spectroscopy (TOF-SIMS). TOF-SIMS was performed on a Physical Electronics TRIFT-III located at the Northwestern University Keck Interdisciplinary Surface Science Center with a liquid Ga ion source. The primary-ion gun was operated at 15 kV and 500 pA in the bunched mode giving a mass resolution for Si of $m/\Delta m = 4000$. Spectra were collected from a 100 μm by 100 μm area with a total primary-ion dose of 2×10^{11} ions/cm^2 in order to remain within the static limit.

X-ray Photoelectron Spectroscopy. XPS measurements were performed using an Omicron ESCA Probe located at Northwestern University Keck Interdisciplinary Surface Science Center with monochromated Al Kα radiation ($h\nu = 1486.6$ eV). The sample was oriented with a 45° photoelectron takeoff angle from the sample surface to the hemispherical analyzer. An analyzer pass energy of 50 eV with 500 meV steps was used for single-sweep survey scans. High-resolution spectra were averaged over three sweeps using an analyzer pass energy of 17 eV with 20 meV steps. Unless otherwise noted, samples were ultrasonicated in CH_2Cl_2 and methanol for 2 min prior to XPS analysis. XPS spectra analyses were performed using XPSPeak 4.1.[22] Peaks were fit with a Gaussian−Lorentzian sum function after a Shirley background subtraction.

Atomic Force Microscopy. AFM imaging was performed with an Autoprobe CP Research AFM using triangular Si Ultralevers with spring constants of approximately 3.2 N/m and nominal tip radii of 10 nm. Unless otherwise noted, all images were collected under ambient conditions at 50% relative humidity and 23 °C with the atomic force microscope operated in intermittent-contact mode.

X-ray Reflectivity. X-ray specular reflectivity measurements were performed on an 18 kW rotating anode, two-circle diffractometer at the Northwestern University X-ray Facility with Cu Kα radiation ($\lambda = 1.542$ Å) operating at 50 kV and 240 mA. An Osmic MaxFlux parabolic multilayer mirror was used as a monochromator. The instrumental resolution for the perpendicular wave vector transfer ($q = 4\pi \sin\theta/\lambda$) was $\Delta q = 5 \times 10^{-3}$ Å^{-1}. After NaI detector dead-time correction and background subtraction, the experimental reflectivity data $R(q)$ were simulated by using the dynamical scattering theory approach based on Parratt's recursion formulation.[23] This approach can be used over the entire collected range of q. The fit parameters were electron density of the film (ρ_F), film thickness (t), respective widths (or roughnesses) of the Si−film (σ_I) and film−air interfaces (σ_S). In addition to this dynamical approach, we also used the kinematical approach to fit the measured reflectivity data normalized to Fresnel reflectivity for an ideal Si mirror $R(q)/R_F(q)$ (details can be found in the Supporting Information). No significant differences were found between the results from these two approaches for XRR analysis.

X-ray Standing Wave and Fluorescence. The XSW and XRF analyses were carried out with the same rotating anode setup as used for the reflectivity measurements. However, to excite Br K fluorescence the Cu target of the rotating anode was replaced by a Mo target, in which case Mo Kα radiation ($\lambda = 0.709$ Å) was used. The XSW was generated by the (111) Bragg diffraction condition from the Si sample substrate. The schematic

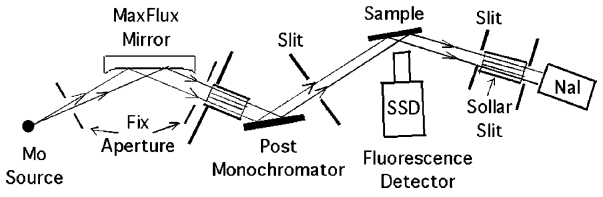

Figure 2. Schematic drawing of the experimental setup used for the XRF and XSW measurements. The XRR setup was identical, except that a Cu rotating anode target replaced the Mo target, there was no single-crystal post monochromator, and there was no SSD fluorescence detector.

drawing for the experiment setup is shown in Figure 2. A Si(Li) fluorescence solid-state detector (SSD) faced the sample. A grazing incidence asymmetric Si(111) crystal with a miscut of 5° was used as a monochromator/collimator for the XSW measurements (this was replaced by a symmetric Ge(111) monochromator crystal for the XRF measurements). For determining the Br coverage, X-ray fluorescence spectra were taken at an incident angle of $\theta = 1.0°$ from SAM-**2**, SAM-**3** and an implanted standard sample.

For the (111) XSW measurement, we simultaneously recorded the X-ray fluorescence spectra and the reflectivity R as a function of angle θ. The normalized Br fluorescence yield Y is given by[19]

$$Y(\theta) = 1 + R(\theta) + 2\sqrt{R(\theta)} f_H \cos[\nu(\theta) - 2\pi P_H] \qquad (1)$$

where ν is the phase of the XSW. Fit parameters f_H and P_H are the coherent fraction ($0 \leq f_H \leq 1$) and coherent position ($0 \leq P_H < 1$), respectively. In general terms, f_H and P_H are the amplitude and phase of the $H = hkl$ Fourier component of the Br distribution. For the simple case of a single adsorption site, the coherent position P_H will be the $\Delta d/d$ fractional d spacing preferred position for that site, and f_H will be the fraction of atoms located at that preferred position.

Throughout all of the X-ray measurements, the samples were sealed within a nitrogen gas flow cell with Kapton windows to avoid oxidation through air exposure. XRR, XRF, and XSW measurements were made as a function of time and as a function of X-ray radiation exposure with the conclusion that there were no structural changes occurring in the SAMs due to time spent in the N_2 cell or due to radiation damage. For the XRR, XSW, and XRF measurements, the respective incident X-ray flux at the sample was 14.7, 0.70, and 0.35×10^7 p/s, the horizontal-by-vertical beam footprint at the sample was $0.25/\sin\theta \times 15.8$, 8.0×5.0, and 8.6×4.0 mm^2, and the collection time for a complete set of data was 4, 7, and 2 h. The samples were $30 \times 17 \times 0.5$ mm^3 in wide-by-high-by-thick dimensions.

Results and Discussion

The TOF-SIMS analyses on samples of SAM-**1** and SAM-**2** support the assertion that UV-irradiation facilitated the reaction between the terminal olefinic groups of **1** and **2** and the hydrogen-terminated Si(111) surface (see the Supporting Information).

High-resolution C_{1s} XPS spectra for H−Si(111), SAM-**1**, and SAM-**2** are shown in Figure 3a−c. The peaks at 284.5, 286.0, and 288.8 eV are assigned to aliphatic carbons, C−O, and C═O functional groups,[8,24] respectively. The observation of the peaks at 284.5 and 286.0 eV on the H−Si(111) sample is attributed to the presence of adventitious hydrocarbons. Further, the relative area of these two peaks on H−Si(111) is much closer to unity than on either SAM-**1** or SAM-**2**. Since all three samples were ultrasonicated in methanol prior to XPS analysis, it is probable that methanol is a significant contaminant on these surfaces. This offers some explanation for the relative abundance of a C−O moiety on the H−Si(111) sample.

(21) Hersam, M. C.; Guisinger, N. P.; Lyding, J. W.; Thompson, D. S.; Moore, J. S. *Appl. Phys. Lett.* **2001**, *78*, 886.

(22) Kwok, R. W. M. Computer code *XPSPeak*, version 4.1; The Chinese University of Hong Kong: Shatin, New Territories, Hong Kong SAR, 1999.

(23) Parratt, L. G. *Phys. Rev.* **1954**, *95*, 1359.

(24) *Handbook of X-ray Photoelectron Spectroscopy*; Chastain, J., Ed.; Perkin-Elmer Corp., Physical Electronics Division: Eden Prairie, MN, 1992; Chapter 1, p 10; Chapter 2, p 98; Chapter 2, p 41.

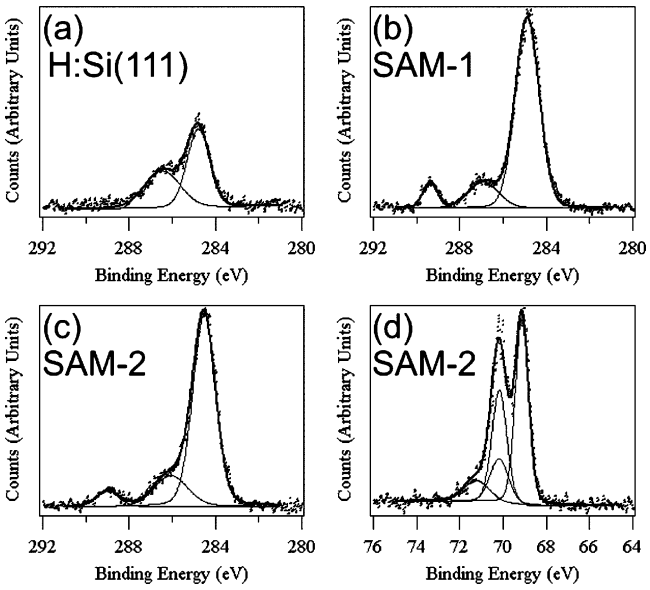

Figure 3. High-resolution XP spectra of H−Si(111) (a), SAM-**1** (b), and SAM-**2** (c,d). The C_{1s} region is shown in parts a−c, and the Br_{3d} region in part d. The carbon spectra show peaks at 284.5, 286.0, and 288.8 eV assigned to the aliphatic, carboxy, and carbonyl carbons, respectively. The carbonyl peak is characteristic of the ester functionality in compounds **1** and **2**. The bromine spectrum shows a convolution of two pairs of spin-doublets at 70.1 and 71.2 eV and at 69.1 and 70.2 eV assigned to carbon- and silicon-bound bromine, respectively.

Further, the C═O peak at 288.8 eV is not observed as a contaminant on the H−Si(111). The much higher relative intensity in the aliphatic carbon peak and the observation of the C═O peak for SAM-**1** and SAM-**2** are consistent with the presence of the predominant aliphatic hydrocarbon ester films.

The high-resolution Br_{3d} XPS spectrum for SAM-**2** is shown in Figure 3d. Bromine was not detected as a contaminant on either H−Si(111) or SAM-**1**. A good curve fit of the Br_{3d} spectrum could not be obtained with only one pair of peaks while maintaining the necessary constraints for the Br_{3d} spin doublet ($\Delta E = 1.05$ eV, 2:3 peak area ratio).[24] By including a second pair of peaks shifted by positive 1 eV from the first pair with the same constraints, a good fit to the spectrum was obtained. This indicates that the Br in SAM-**2** exists in two different oxidation states. The two pairs of peaks are attributed to Si−Br and C−Br bonding configurations. Further explanation for the Si−Br bond assignment is discussed later. Because C is more electronegative than Si, the C−Br bond should be shifted to a higher binding energy than the Si−Br bond. Thus, the higher energy spin doublet at 70.1 and 71.2 eV is assigned to C−Br, and the lower energy spin double at 69.1 and 70.2 eV is assigned to Si−Br. It is further observed that the relative abundance of Si−Br is greater than that of C−Br. A quantitative comparison of these peak areas is not very reliable, due to the significant overlap of the peaks at 70.1 and 70.2 eV.

AFM topography images of H−Si(111), SAM-**1**, and SAM-**2** are shown in Figure 4a−c. The step morphology of the hydrogen-passivated Si surface is maintained for the SAMs. This is consistent with previous observations for alkyl monolayers[7] and indicates that the ester functionality does not impede the growth of a densely packed monolayer. The small round topographical features decorating the atomic steps in all three images are attributed to incipient oxidation that occurs during the final water rinse in the hydrogen-passivation process.

Figure 5 shows the measured specular X-ray reflectivity for the H−Si(111), SAM-**1**, and SAM-**2** samples. The solid lines are theoretical fits using Parratt's recursion formulation.[23] Unlike the Fresnel-like decay of the H−Si(111) surface, the samples with organic films show clear interference thickness oscillations. The best reflectivity fit for the H−Si(111) sample has a surface roughness of 4 Å, which is typical for Si.[5,6,14,25] The reflectivities from both SAM-**1** and SAM-**2** were simulated with a one-layer model. Including a very thin, higher electron density second layer to model the Br atoms did not improve the fit for the SAM-**2** data. A more detailed discussion for this sample will be given later. The appearance of the interference minimum at a slightly lower value of q for the SAM-**2** sample indicates that it has a slightly thicker film than the SAM-**1** monolayer. Table 1 shows the results for the Parratt one-slab reflectivity analysis shown in Figure 5. Our XRR-determined SAM-**1** film thickness of 12.2 Å is close to the 13 Å that was reported[5] for an undecylenic acid methyl ester monolayer grown at 200 °C without UV on an HF-etched Si(001) surface. (The data from this earlier result reportedly "could not be measured accurately, because of a considerable contribution of the background to the signal for $q > 0.35$ Å^{-1}".[5])

Table 1 also lists our calculated molecular tilt angles (α) and coverages (Θ) for the two different SAMs on the Si(111) surface. For SAM-**1**, the tilt angle α and coverage Θ were calculated from the XRR-measured values for ρ_F and t, along with the known number of electrons in SAM-**1** ($Z = 110$) and molecular length[26] ($L = 15.5 \pm 0.1$ Å). Accordingly, the tilt angle α is equal to $\cos^{-1}(t/L) = 38°$ for SAM-**1**, and the coverage Θ is equal to $\rho_F/(Z/At) = 0.50$ monolayer (ML), where $A = 12.77$ Å^2 is the area per Si surface atom on an ideal Si(111) surface. The XRR-measured 0.50 ML coverage for SAM-**1** is close to the maximum coverage observed[4,5,27] for alkyl chains on a Si(111) surface. This limiting coverage is considered to be primarily due to steric hindrance effects where two 4.6 Å diameter[5] molecules cannot fit on neighboring Si atomic surface sites because of the 3.84 Å spacing between the hexagonal array of Si surface atoms. We will discuss later how we estimated the SAM coverage and molecular tilt angle for SAM-**2**. For comparison, we used the kinematical approach to fit the normalized reflectivity data from SAM-**1** and SAM-**2** (see the Supporting Information for details). The fit parameters from this approach were found to be equivalent to the dynamical approach values listed in Table 1, indicating the suitability of the one-layer model for characterizing the reflectivity for these two SAMs and the reliability of the fit parameters.

The XRF-determined total Br coverage of $\Theta_{Br} = 0.58 \pm 0.04$ ML was measured by comparing the Br Kα fluorescence yield from SAM-**2** to the As Kα yield from an arsenic ion implanted Si(111) standard sample that had a coverage calibrated by Rutherford backscattering spectrometry (RBS). (At $E_\gamma = 17.479$ keV, the Br Kα to As Kα fluorescence yield per atom is 1.33 ± 0.02.[28])

The results for the single-crystal XSW measurement using Si(111) Bragg diffraction are presented in Figure 6.[29] The coherent position and fraction obtained from the fit of eq 1 to the data are $P_{111} = 0.83 \pm 0.02$ and $f_{111} = 0.82$

(25) Zhu, X. Y.; Boiadjiev, V.; Mulder, J. A.; Hsung, R. P.; Major, R. C. *Langmuir* **2000**, *16*, 6766.
(26) *CS ChemBats3D Pro*, version 4.0; CambridgeSoft Corp.: Cambridge, MA, 1997.
(27) Sieval, A. B.; Hout, B. van den; Zuilhof, H.; Sudhölter, E. J. R. *Langmuir* **2001**, *17*, 2172.
(28) Criss, J. W.; Birks, L. S.; Gilfrich, J. V. (Computer program NRL XRF) *Anal. Chem.* **1978**, *50*, 33.

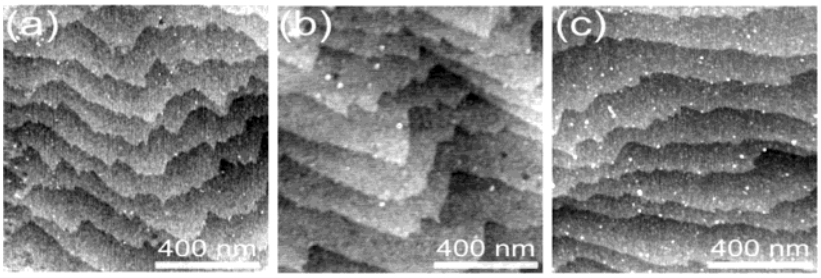

Figure 4. AFM topography images of (a) H−Si(111), (b) SAM-**1**, and (c) SAM-**2**, showing that the step morphology of the hydrogen-passivated silicon surface is maintained.

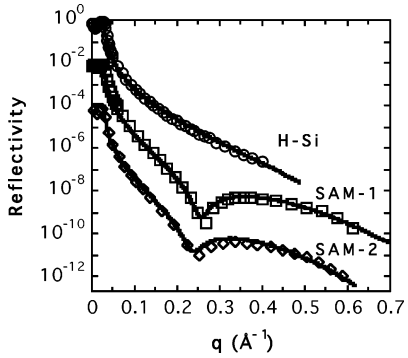

Figure 5. X-ray specular reflectivity data (circles, squares, and triangles) from samples H−Si(111), SAM-**1**/Si(111), and SAM-**2**/Si(111). The solid lines are theoretical fits by Parratt's method using a one-layer model. The structural parameters from this fit are listed in Table 1. For clarity, successive data sets are displaced by a factor of 100.

Table 1. XRR One-Layer Model Determined Film Electron Density (ρ_F), Film Thickness (t), Si−Film Interface Roughness (σ_I), and Film−Air Interface Roughness (σ_S)[a]

sample	ρ_F (e$^-$/Å^3)	t (Å)	σ_S (Å)	σ_I (Å)	α (deg)	coverage Θ (ML)
H−Si(111)	0	0		4.0(2)		0
SAM-**1**	0.35(2)	12.2(2)	2.3(2)	3.2(2)	38(4)	0.50(4)
SAM-**2**	0.37(2)	13.2(2)	3.0(2)	3.6(2)	23(2)	0.57(4)
SAM-**3**	0.12(2)	12.2(2)	1.6(2)	6.4(2)	30(2)	0.13(3)

[a] The calculated molecular tilt angle (α) and SAM coverage (Θ) are based on t and ρ_F along with the attached molecular length (ref 27) for SAM-**1** and SAM-**2**.

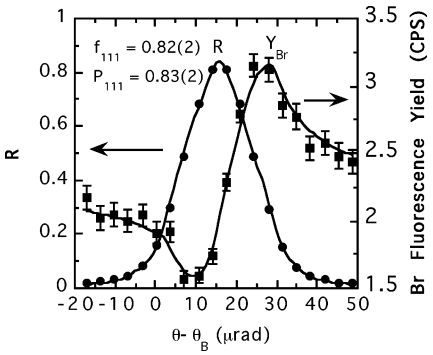

Figure 6. Single-crystal XSW results for the SAM-**2** on Si(111) sample. Shown are the angle dependence of the Si(111) Bragg reflectivity (R) "rocking curve" and the Br Kα fluorescence yield data. Symbols are measured data, and solid lines are best-fits of theory (including eq 1) to the data.

± 0.02, respectively. Interestingly, to within the 0.05 Å uncertainty of the measurement, this coherent position for Br is identical to earlier measured coherent positions for Br for the cases in which Br was adsorbed from a methanol solution[18] and in ultrahigh vacuum (UHV)[30] onto a Si(111) surface. In both cases,[18,30] the monatomic Br was triangulated to be at the T_1 site with a height corresponding to the expected height for an unstrained, bulklike positioned Si surface atom bonded to Br with h = 2.17 Å, which is equivalent to the summed covalent radii of Br and Si. This, in conjunction with the Br XPS analysis (Figure 3d), confirms that most of the Br has been removed from **2** during SAM-**2** preparation and has covalently bonded to the Si(111) surface. The high coherent fraction value of 0.82 indicates the fraction of Br atoms that exist in this arrangement.

Combining the XRF and XSW results, we can compute the Br "coherent coverage" as $f_{111}\Theta_{Br} = 0.48 \pm 0.04$ ML. This indicates that one-half of the Si dangling bond sites are terminated with Br. The remaining 0.10 ML of Br have a distribution width in the [111] direction that is greater than 2 Å and therefore appear randomly distributed relative to the (111) XSW which has a period of d_{111} = 3.135 Å. If the random distribution of Br is in the monolayer film, it would suggest that the bromoethoxy moiety present in SAM-**2** is not packed rigidly. Note that this XSW 0.5−0.1 ML partitioning of the Br is in general agreement with the Br XPS Si−Br to C−Br partitioning shown in Figure 3d, which further substantiates our conclusions concerning the final bonding configuration of Br.

We can now more perceptively interpret the ρ_F and t values from the one-layer model fit to the SAM-**2** reflectivity data. The 1/2 ML of Br at the interface has essentially the same electron density as bulk Si. Therefore, the XRR-measured thickness value of $t = 13.2 \pm 0.2$ Å corresponds to the height difference between the top of the SAM and the top of the Br layer which is ∼2.2 Å above the top Si atom. This vertical separation of $t' \sim 15.4 \pm 0.2$ Å between the top Si atom and the top atom in the SAM can be used to calculate the molecular tilt angle α and the SAM coverage Θ. However, for these calculations we need to know the chemical composition of the SAM at the interface. From the XSW analysis, it is clear that at most 0.1 ML of **2** is bound to the Si surface as depicted in Figure 7A. The presence of 0.5 ML of Br bound directly to the Si surface indicates that some decomposition of **2** has occurred during SAM preparation. As an initial estimate, we consider the case where Br abstraction leads to an ethyl ester terminated SAM (Figure 7B). The calculated

(29) Unlike typical XSW data, these data were collected on a conventional X-ray source with a conventional single-side-polished CZ-grown thin Si wafer. The data could have been much more rapidly collected at a synchrotron X-ray beamline. And the data could have had a sharper reflectivity curve and XSW modulation if a FZ-grown, thick, strain-relieved, Si sample were used. However, in this case the Br Kα emission rate is sufficient to allow us to collect the data in-house and the theory (eq 1) can be appropriately convoluted to fit the data and extract the f and P values with sufficient accuracy.

(30) Funke, P.; Materlik, G. *Surf. Sci.* **1987**, *188*, 378.

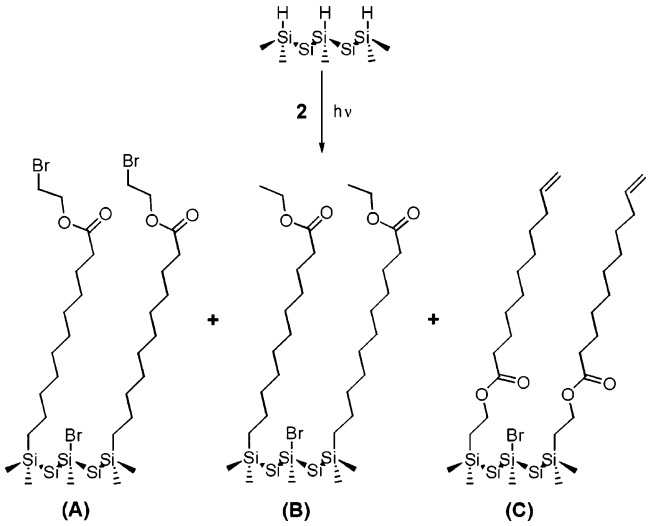

Figure 7. Schematic representation of the process to prepare SAM-**2** attachment to the Si(111) surface. Based on the XSW, XRF, and XPS measurements, the process produces 0.50 ML of Br covalently bonded to Si(111) T_1 sites. The organic film is composed of **2** bound in the following configurations: (A) ≤0.10 ML, (B) ≥0.27 ML, and (C) ≤0.13 ML.

molecular length for this configuration is 16.7 Å,[26] resulting in a molecular tilt angle $\alpha = 23°$ and $\Theta = 0.57$ ML.

To investigate the possible photolability of Br from **2** under our conditions for SAM preparation, **2** was irradiated with UV light in the absence of H−Si(111). It was postulated that UV-induced homolytic cleavage of the CH_2−Br bond in **2** would result in decomposition of the starting material. However, characterization of irradiated samples by ^{1}H NMR and GC provided no evidence of such decomposition. Therefore, we conclude that Br abstraction from **2** is initiated by Si surface radicals formed during UV irradiation of the H−Si(111) surface.[6]

Abstraction of Br from **2** at the Si surface during SAM-**2** preparation generates a terminal methylene radical, providing an alternate reactive site in the molecule for reaction with the Si surface. Two scenarios are proposed as illustrated in Figure 7B,C. In case B, the methylene radical abstracts hydrogen from a neighboring Si−H group resulting in a terminal ethyl ester. Chemisorption of the ethyl ester proceeds via reaction of a Si radical with the terminal olefin, producing the ethyl ester terminated surface shown in Figure 7B. A similar mechanism for hydrogen abstraction from Si−H by alkyl radicals has been proposed for the electrochemical derivitization of H-terminated porous Si with 1-haloalkanes.[31] Alternatively, the methylene radical formed upon Br abstraction by the Si surface can react directly with another Si surface radical resulting in an alkenyl-terminated surface (Figure 7C). A similar reaction mechanism has been proposed for the chemisorption of 1-haloalkanes with clean Si(100) and (111) in UHV,[32,33] with scribed silicon,[17,34] and with H-terminated porous silicon.[31]

While it is clear from the XSW results that at least one of these reaction pathways is active (i.e., at most 0.1 ML of Br is present within the 0.5 ML film), it is not clear

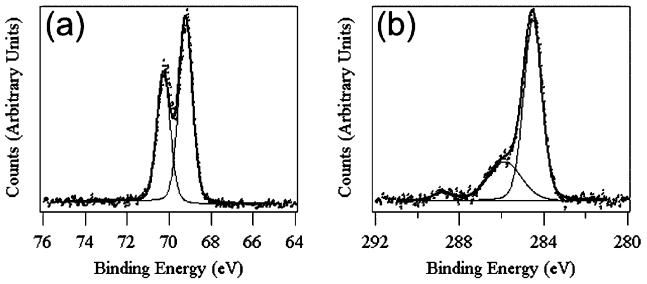

Figure 8. High-resolution XP spectra of the H−Si surface prepared with compound **3**. The Br_{3d} spectrum (a) contains a single spin-doublet pair at 69.2 and 70.3 eV assigned to silicon-bound bromine. The absence of the carbon-bound bromine spin doublet at 70.1 and 71.2 eV is noted. The C_{1s} spectrum (b) shows peaks at 284.5, 285.8, and 288.7 eV assigned to the aliphatic, carboxy, and carbonyl carbons, respectively. The presence of the carbonyl peak indicates that **3** is reactive with the H−Si surface.

which of the proposed binding configurations is present. To investigate this, an H−Si(111) surface was immersed in compound **3** (see Chart 1) and irradiated with UV light under our conditions for SAM preparation. Because molecule **3** lacks a terminal olefin, any reaction with the Si surface is expected to occur through the methylene radical generated upon Br abstraction (vide supra). The high-resolution Br_{3d} and C_{1s} XPS spectra for the surface prepared with **3** are shown in Figure 8a,b. A good fit of the Br_{3d} spectrum was obtained using one pair of peaks at 69.2 and 70.3 eV. This spin doublet has been assigned to Br bound to Si (vide supra). The absence of the C−Br spin doublet at 70.1 and 71.2 eV is noted. The C_{1s} spectrum contains peaks at 284.5, 285.8, and 288.7 eV which have been assigned to aliphatic carbon, C−O, and C═O, respectively (vide supra). The carbonyl peak at 288.7 eV indicates the presence of **3** on the surface. This could be due either to physisorbed material that was not successfully removed during cleaning or to chemisorbed **3**. Due to the absence of any substantial C−Br bonds on the surface, we believe that the carbonyl peak is most likely due to chemisorbed **3** bound as shown in Figure 7C. The C/Si ratio for the carbonyl peak for the surface prepared with **3** is about 1/3 of that of SAM-**2**.

Table 1 shows the results for the Parratt one-slab reflectivity analysis of the specular X-ray reflectivity measured from an H−Si(111) surface prepared with **3**. The best fit of the measured data indicates a film thickness of 12.2 Å and an electron density of 0.12 e^-/Å^3. The calculated molecular tilt angle (α) and coverage (Θ) for SAM-**3** are listed in Table 1. The tilt angle for SAM-**3** is lower than that of the more densely packed SAM-**1**. Previous studies of self-assembled monolayers prepared from allyl esters on H−Si(100) report that the presence of an ester group near the silicon surface results in a more disordered monolayer.[5] These authors attribute this to steric hindrance by the ester group inhibiting the approach of alkenes to neighboring Si atoms. This report is consistent with the low coverage calculated for SAM-**3**. Furthermore, steric hindrance due to the ester group positioned near the silicon surface may explain the lower tilt angle observed for this SAM.

From the XPS and XRR measurements, we estimate the coverage of **3** to be 0.13 ML. This suggests that a reasonable maximum content of **2** bound in the Figure 7C configuration in SAM-**2** is 0.13 ML, assuming steric hindrance is the limiting factor for packing density. From these results, it is apparent that the sum of **2** bound in the Figure 7A,C configuration, 0.1 and 0.13 ML, respectively, cannot account for the total 0.5 ML coverage in

(31) Gurtner, C. G.; Wun, A. W.; Sailor, M. J. *Angew. Chem., Int. Ed.* **1999**, *38*, 1966.
(32) Keeling, L. A.; Chen, L.; Greenlief, C. M.; Mahajan, A.; Bonser, D. *Chem. Phys. Lett.* **1994**, *217*, 136.
(33) Klug, D. A.; Greenlief, C. M. *J. Vac. Sci. Technol., A* **1996**, *14*, 1826.
(34) Niederhauser, T. L.; Lua, Y.-Y.; Sun, Y.; Jiang, G.; Strossman, G. S.; Pianetta, P.; Linford, M. R. *Chem. Mater.* **2002**, *14*, 27.

SAM-**2**. Based on these estimates, it is probable that all three of the bonding configurations for **2** depicted in Figure 7A−C are present in SAM-**2**, with configuration B being dominant, making up at least 0.27 ML of the ∼0.5 ML organic film.

Summary

Our results show that densely packed SAMs of **1** and **2** have been successfully formed on hydrogen-passivated Si(111) surfaces. X-ray specular reflectivity, XPS, AFM, TOF-SIMS, X-ray fluorescence, and Si(111) Bragg diffraction X-ray standing waves have proven to be a unique, powerful, and complementary set of probes for quantitatively characterizing the SAMs on an atomic scale. The results reveal that the monolayers have a 0.5 ML surface saturation coverage equivalent to that of alkyl chains on Si(111). The monolayers are tilted at 38° for SAM-**1** and 23° for SAM-**2** from the substrate surface normal. Both the olefinic and bromoethyl moieties of **2** are reactive at the H−Si(111) surface under UV irradiation leading to 0.5 ML of Br covalently bound to Si and 0.5 ML of a predominantly ethyl ester terminated SAM. The Br layer covalently bonded to the Si at the SAM/Si(111) interface can serve as a convenient reference marker layer for long-period XSW[35,36] *z*-profiling of subsequent chemical modifications of the SAMs which include molecules containing other heavy atoms, such as modified-DNA and immobilized catalysts. More generally, a strategy has been demonstrated for characterizing the film composition of SAMs prepared from molecules containing multiple reactive groups.

Acknowledgment. The authors acknowledge support from the Nanoscale Science and Engineering Initiative of the National Science Foundation under NSF Award Number EEC-0118025, the National Institutes of Health under Contract Number GM62109-02, the Rockefeller Brothers Fund, and the Northwestern University Institute for Bioengineering and Nanoscience in Advanced Medicine. This work made use of Central Facilities supported by the MRSEC program of the National Science Foundation (DMR-0076097) at the Materials Research Center of Northwestern University and of the Keck Interdisciplinary Surface Science Facility which is supported by the Nanoscale Science and Engineering Center of Northwestern University. One of the authors (C.R.K.) acknowledges funding from a National Defense Science and Engineering Graduate Fellowship.

Supporting Information Available: TOF-SIMS results and discussion containing a high-resolution scan of the 1-bromoethyl fragment and the fit of eq 2 to normalized data. This material is available free of charge via the Internet at http://pubs.acs.org.

LA0496690

(35) Bedzyk, M. J.; Bilderback, D. H.; Bommarito, G. M.; Caffrey, M.; Schildkraut, J. S. *Science* **1988**, *241*, 1788.

(36) Bedzyk, M. J.; Bommarito, G. M.; Schildkraut, J. S. *Phys. Rev. Lett.* **1989**, *62*, 1376.